

Prediction of temperature distribution in turbulent Rayleigh-Benard convection

Zhen-Su She,* Xi Chen, and Jun Chen

*State Key Laboratory for Turbulence and Complex Systems and Department of Mechanics,
College of Engineering, Peking University, Beijing 100871, China*

Hong-Yue Zou and Yun Bao

*State Key Laboratory for Turbulence and Complex Systems and Department of Mechanics,
College of Engineering, Peking University, Beijing 100871, China and
Department of Mechanics, College of Engineering,
Sun Yat-sen University, Guangzhou, 510275, China*

Fazle Hussain

*State Key Laboratory for Turbulence and Complex Systems and Department of Mechanics,
College of Engineering, Peking University, Beijing 100871, China and
Department of Mechanical Engineering, University of Houston, Houston, TX 77204-4006, USA
(Dated: July 23, 2021)*

A quantitative theory is developed for the vertical mean temperature profile (MTP) in turbulent Rayleigh-Benard convection (RBC), which explains the recent experimental and numerical observations of a logarithmic law by Ahlers et al. [1]. A multi-layer model is formulated and quantified, whose predictions agree with DNS and experimental data for the Rayleigh-number (Ra) over seven decades. In particular, a thermal buffer layer follows a $1/7$ scaling like the previously postulated mixing zone [2], and yields a Ra -dependent log law constant. A new parameterization of $Nu(Ra)$ dependence is proposed, based on the present multi-layer quantification of the bulk MTP. .

Turbulent Rayleigh-Benard convection (RBC) is a well-known non-equilibrium system displaying rich dynamics of both fundamental interest and wide technological relevance [3–5]. Numerous results have been obtained experimentally and numerically, while the theoretical understanding remains relatively poor. For instance, a diverse set of heat flux measurements [6, 7] are yet to be explained; the origin of observed "classical state", "transition range" and "ultimate state" [8] remains elusive. Recently, efforts begin to be directed to the study of the structure of the thermal boundary layers and of bulk non-vanishing temperature gradient (see, for instance, [17, 18]), but no accurate prediction of the full MTP is available. Very recently, Ahlers et al. [1] found, beyond the thin boundary layer unresolved in the experiment, that the temperature and its root-mean-square (rms) fluctuation vary logarithmically as a function of the distance z from the bottom plate. Grossman and Lohse [9] have developed an argument for the logarithmic mean temperature with an assumption of kinetic logarithmic layer, but offer few quantitative predictions. It is clear that a theory of RBC needs to go beyond the estimates of global quantities [10] and predict internal temperature distribution. The recent finding of Ahlers et al. [1] represents a significant effort in this direction.

Here, we develop a theory of MTP, based on a new mean-field approach applying a symmetry analysis to wall-bounded turbulent flows [11] which yields accurate predictions of the mean velocity profile over a wide range of Reynolds number [12]. Here, it is shown that this mean-field theory yields a valid description of the MTP in RBC, including, in particular, the log law with coefficients quantitatively validated by data for Ra over seven decades. An intriguing outcome is that a thermal buffer layer thickness is found to vary as $Ra^{1/7}$, exactly like that of earlier speculated mixing zone [2].

The temperature variation in fully developed RBC is described by the Boussinesq equations [13],

$$\kappa \frac{\partial^2 \Theta}{\partial z^2} - \frac{\partial \langle w\theta \rangle}{\partial z} = 0 \quad (1)$$

where θ denotes temperature re-scaled by the total temperature difference Δ , and equals $\pm 1/2$ on the bottom ($z = 0$) and top ($z = 1$) plates, and $\langle \dots \rangle$ denotes time and space average except in the vertical z direction (i.e. $\Theta = \langle \theta \rangle$); κ is the thermal diffusivity, w is the vertical velocity, carrying all information about turbulent fluctuations. Integrating (1) along z once yields the mean temperature equation (MTE) [13]:

$$-\frac{d\Theta}{dz} + \frac{\langle w\theta \rangle}{\kappa} = -\frac{d\Theta}{dz} \Big|_{z=0} \equiv Nu \quad (2)$$

*Electronic address: she@pku.edu.cn

Denote $S_\theta^+ = -d\Theta/(Nudz) = -d\Theta/dz^+$ and $W_\theta^+ = \langle w\theta \rangle / (\kappa Nu) = \langle w^+\theta \rangle$, Then, the normalized MTE is

$$S_\theta^+ + W_\theta^+ = 1 \quad (3)$$

with normalized vertical coordinate, $z^+ = zNu$ and vertical velocity, $w^+ = w/(\kappa Nu)$.

It is interesting to compare (3) to the mean momentum equation (MME) in a pipe or channel [14]: $\nu dU/dy - \langle uv \rangle = u_\tau^2(1 - y)$ with friction velocity u_τ , and kinematic viscosity ν . The MME can be rewritten in wall units:

$$S^+ + W^+ = \frac{dU^+}{dy^+} - \langle uv \rangle^+ = 1 - y^+/\text{Re}_\tau \quad (4)$$

where $U^+ = U/u_\tau$, $W^+ = -\langle uv \rangle^+ = -\langle uv \rangle / u_\tau^2$, $y^+ = yu_\tau/\nu$ the distance to the wall, $\text{Re}_\tau = u_\tau H/\nu$ with $H = 1$ being the half width of a channel. In the so-called overlap region at high Re_τ , $y^+ \ll \text{Re}_\tau$, $S^+ + W^+ \approx 1$, which is exactly the same as (3). Thus, we identify similarities between (3) and (4) in three aspects: first, near the wall, both S^+ and S_θ^+ dominate and equal to unity; second, away from the wall, W^+ and W_θ^+ dominate and equal to unity; third, W^+ and W_θ^+ both represent effect of transport by velocity fluctuations normal to the wall. Thus, we postulate a system similarity between the momentum and temperature (energy) and suggest that the distribution of the mean temperature follows the same symmetry as the mean momentum.

Recently, a symmetry-based theory is developed for S^+ , giving rise to a quantitative description of the mean velocity distribution [11, 12], assuming a dilation-group invariance of the mixing length, $\ell_M^+ = \sqrt{W^+}/S^+$. In analogy to order parameter displaying a symmetry change during a phase transition, the mixing length is called order function, which characterizes the far-from-equilibrium state of turbulent wall-bounded flow in terms of multiple scaling symmetries occurring in different domains. Specifically, wall-bounded turbulence forms several layers, called viscous sublayer, buffer layer, bulk flow etc., each of which is occupied by fluctuations of distinct scaling (dilation invariance). The Lie-group analysis is an effective tool to quantify such a multi-layer structure, yielding an accurate description from S^+ -dominant boundary to W^+ -dominant bulk. The system similarity assumption guides a similar description for Θ , by defining a thermal mixing length:

$$\ell_\theta^+ = \sqrt{W_\theta^+}/S_\theta^+ \quad (5)$$

which is assumed to display the same symmetry property as ℓ_M^+ .

Note that the dimension of ℓ_θ (the absence of superscript '+', denotes no normalization) is no longer length, so its meaning needs to be interpreted. We follow Prandtl's original apt argument that the effect of a fluctuating velocity on the transport of a mean "density" (momentum or energy) can be represented by an eddy viscosity, $W = \nu_t S$, W being the Reynolds stress, $\nu_t = \ell_M^2 S$ and ℓ_M have the right dimensions of viscosity and length. In the case of temperature, $\nu_\theta = W_\theta/S_\theta$ has still the dimension of diffusivity, but a dimensionally correct expression for ν_θ should be $\nu_\theta = \ell_\theta^2 S = \ell_\theta^2 S_\theta (S/S_\theta) = \ell_\theta^2 S_\theta \Omega$, where we introduce a dimensional quantity $\Omega = S/S_\theta$, by substituting S (velocity gradient or mean shear rate) by S_θ (temperature gradient). The system similarity is valid if $\Omega \equiv \text{Const}$, or ℓ_θ plays the same role for the convective heat transport as ℓ_M for momentum transport. This is sound at least when the turbulent Prandtl Number is unity, because the turbulent velocity and temperature fluctuations and the corresponding momentum and energy transports being due to the same fluid motion.

Whether ℓ_θ is an order function is ultimately tested against empirical data, by the criterion that it characterizes multiple scaling states of varying symmetry (or dilation invariance). The DNS for RBC is performed in a narrow rectangular box with aspect ratios of X:Y:Z=6:1:6, where x, y, z denote horizontal, spanwise and vertical directions, respectively (aspect ratio $\Gamma = 1$). Thermal convection takes place essentially in the x and z planes, with developed spanwise motions enriching 3-D dynamics. The simulation is performed using a finite-difference solver of the standard Navier-Stokes equation under Boussinesq approximation coupled to thermal advection-diffusion equation. Two simulations are done at $Ra = 10^8$ and 10^9 , and ℓ_θ is computed using (5) and shown in Fig.1. The three layers (sublayer, buffer and log layers) are clearly displayed, while we ignore the last one near the centre for simplicity, which contribute little at high Ra . In this approximation, the classical laminar thermal boundary layer view of RBC at this rather moderate Ra is replaced by a three-layer picture.

Now, we quantify the three-layer temperature variation by postulating a similar (thermal) sublayer, buffer layer and a log layer, for which ℓ_θ displays distinct scalings in z . Specifically, $\ell_\theta^+ \propto (z^+)^{3/2}$ for $z^+ < z_{sub}^+$; $\ell_\theta^+ \propto (z^+)^{5/2}$ for $z_{sub}^+ < z^+ < z_{buf}^+$; and $\ell_\theta^+ \propto z^+$ for $z^+ > z_{buf}^+$. The first exponent (3/2) readily follows from a near-wall expansion with small fluctuations, and the third linear scaling corresponds to the (postulated) log layer. However, the thermal buffer layer has a different scaling increment of one, instead of 1/2 for the momentum buffer-layer, reflecting possibly new form of the near wall temperature fluctuation structure compared to coherent structures of momentum fluctuations.

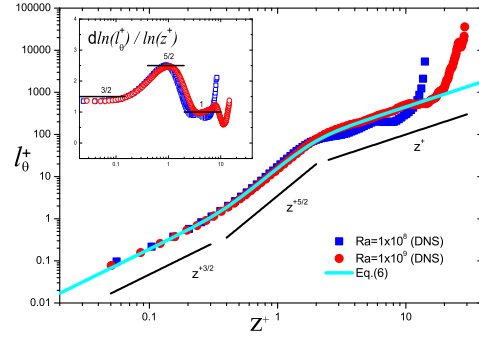


FIG. 1: (color). The variation of the “Mixing length order function” with the normalized vertical distance from the bottom plate. Symbols are our DNS data at two Ra , and line is the model (6) at $Ra = 10^9$ with $\rho \approx 6$, $z_{sub}^+ \approx 0.375$ and $z_{buf}^+ \approx 2$. The inset shows the diagnostic function $d \ln(\ell_\theta)/d \ln(z)$ displaying the local scaling exponents of $3/2$, $5/2$ and 1 for the thermal sublayer, buffer and log layer being, respectively.

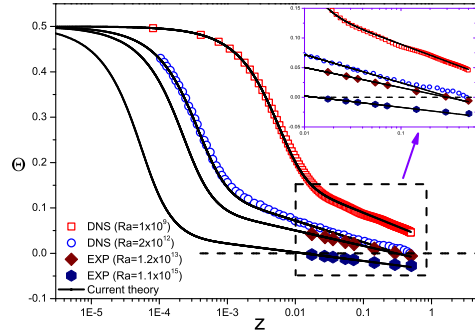


FIG. 2: (color). Predicted MTP from (6) and (7) compared to four sets of empirical data: DNS at moderate- Ra (red squares), DNS at high- Ra (blue diamonds), and two sets of experimental data at very high Ra (filled symbols). Data other than the lowest Ra DNS ones are provided by Ahlers [1]. The inset shows the enlargement showing agreement of the log profiles in the bulk region.

While its nature needs further elucidation, the exponent $5/2$ is empirically confirmed by our DNS data using a Lie-group diagnostic function [12], shown in the inset of Fig. 1. Thus, our system similarity hypothesis yields a composite formula for ℓ_θ^+ as:

$$\ell_\theta^+ \approx \rho (z^+)^{\frac{3}{2}} \left(1 + \left(\frac{z^+}{z_{sub}^+} \right)^4 \right)^{\frac{1}{4}} \left(1 + \left(\frac{z^+}{z_{buf}^+} \right)^4 \right)^{-\frac{3}{8}} \quad (6)$$

where the two transition sharpness parameters are pre-set to be 4 (positive integer), following [12]. Jointly solving (3), (5) and (6) yields a theoretical MTP as

$$\frac{1}{2} - \Theta(z^+) = \int_0^{z^+} S_\theta dz' = \int_0^{z^+} \frac{1 - \sqrt{4\ell_\theta^{+2} + 1}}{2\ell_\theta^{+2}} dz' \quad (7)$$

The first consequence of the theory is the logarithmic profile. For $z^+ \gg z_{buf}^+$, $\ell_\theta^+ \approx \kappa_\theta z^+ \gg 1$, then $S_\theta^+ \approx 1/(\kappa_\theta z^+)$, a logarithmic MTP follows:

$$\Theta \approx -\frac{1}{\kappa_\theta} \ln z^+ + B^+ \approx -A \ln z + B \quad (8)$$

$$\kappa_\theta = \rho z_{buf}^{+3/2} / z_{sub}^+ \quad (9)$$

where coefficients A and B are measured by Ahlers et al. [1]. So, κ_θ ($= 1/A$) depends on Ra through three parameters - the central topic investigated below.

The first two parameters specify the thicknesses of the thermal sublayer and buffer layer, and the third is a global coefficient determining a Karman-like coefficient. The two thicknesses characterize the transition between different scaling ranges, and can be roughly obtained by inspecting Fig. 1: $z_{sub}^+ \approx 0.35$, $z_{buf}^+ \approx 2$ at our moderate Ra . We choose a fixed $z_{sub}^+ \approx 0.375$, as expected for an Ra -independent sublayer in thermal boundary units, and then adjust z_{buf}^+ and ρ for matching the bulk behaviour, e.g. A and B in (8), to yield a prediction of the MTP. Fig. 2 shows the comparison between the theoretical profiles with empirical data for Ra covering seven decades, from moderate (10^8) in DNS to very high (10^{15}) in Gottingen experiments [1]. The agreement is very satisfactory.

Note that the theory, initially developed for horizontally averaged MTP, is validated as shown in Fig. 1. The agreement in Fig. 2 shows that it is also valid for MTP at a fixed location near the sidewall ($x_p = 0.0045$), with the same z_{sub}^+ and slightly different z_{buf}^+ and ρ . Analysis of MTPs at different x locations in our DNS data shows that z_{buf}^+ and ρ have sensitive dependence on x that reveals internal mean-field structure of the momentum and temperature, which will be reported elsewhere. Note also that a common $z_{sub}^+ \approx 0.375$ yields a good description of both our DNS with rectangular geometry and the cylindrical one [1], as expected for universal near-wall variations.

Variation of the fitted z_{buf}^+ and ρ with Ra (Fig. 3) reveals three transitions at $Ra_{c1} \approx 4 \times 10^{11}$, $Ra_{c2} \approx 2 \times 10^{13}$ and $Ra_{c3} \approx 8 \times 10^{14}$. The first plateau in Fig. 3 reveals the presence of weakly turbulent state close to the sidewall at $x_p \approx 0.0045$ for $Ra < Ra_{c1}$. For $Ra > Ra_{c1}$, z_{buf}^+ and ρ begin to vary, indicating that strong fluctuations reach the probe. In all cases, we observe a logarithmic MTP, but with no indication of a kinetic logarithmic layer at moderate $Ra \sim Ra_{c1}$. The second and the third transitions coincide with those reported by [1], indicating that the multi-layer parameters are sensitive to the variation of the physical states. As shown in Fig. 3, we find, for $Ra > Ra_{c1}$, z_{buf}^+ and ρ follow the power-law scaling:

$$z_{buf}^+ \approx 0.031 Ra^{0.143}, \quad \rho \approx 32.1 Ra^{-0.052} \quad (10)$$

where the coefficients are obtained with a least-squares fitting. The variation of z_{buf}^+ is mostly responsible for observed systematic variation of the slope (A), the inverse of which for shear flow is called the Karman constant.

The scaling exponent close to $1/7$ in z_{buf}^+ was predicted by Proccacia et al. [2] based on a earlier proposal of a mixing zone by the Chicago group [15], and experimentally detected by Xia et al. [16]. Thus, we speculate that an increasing buffer layer thickness is a sign of increasing influence of the energetic thermal plumes on the BL. Furthermore, we consider z_{buf}^+ to be a candidate measure of the height of the plumes. This idea should be subjected to further tests by experimental and DNS data. At this point, we caution about the universality of the empirical laws (10) derived here from measurements at a fixed distance from the sidewall [1]; variations of z_{buf}^+ and ρ need further study.

From (9) and (10),

$$\kappa_\theta = 1/A \approx 0.47 Ra^{0.162} \quad (11)$$

This predicts a significant variation of the log-law slope in RBC, as compared to the universal Karman constant in the momentum transfer. Our analysis shows that this variation is primarily due to the change in z_{buf}^+ , interpreted above as the gradual increase of the plume height with Ra . The last transition to the ultimate state is characterized by a rapid decrease of ρ , leading to an overall decrease of ℓ_θ (at all distances from the wall). We interpret this as a sign of plume correlation length crisis: for $Ra > 8 \times 10^{14}$, at the ultimate state, motions become significantly more turbulent, so that a stronger temperature gradient is formed near the wall with a larger asymmetry of the bulk temperature. The exact nature of this crisis needs further investigation.

In summary, we offer the first analytic model for the temperature distribution in the RBC, which is visibly superior to prior models giving temperature variations only in the near-wall region (see [17, 18]). The theory captures the documented small (logarithmic) variation and slight asymmetry of the mean temperature in the bulk of the RBC cell, with a simple postulate of the multi-layer scaling symmetry. Further interpretation will be more intriguing: for instance, a new formula for Nu can be derived from the log-law for θ :

$$Nu \approx A Ra^{1/7} \exp\{(Ra/Ra_c)^\beta\}, \quad (12)$$

which seems to yield a sensitive parameterization to interpret Nu -measurements from different groups (to be reported). On the theoretical ground, further characterization of detailed horizontal dependence would form a complete mean-field theory for the RBC system. Finally, note that the successes reported here and elsewhere [19, 20] support the view that the multi-layer picture is universal to all wall-bounded turbulent flows.

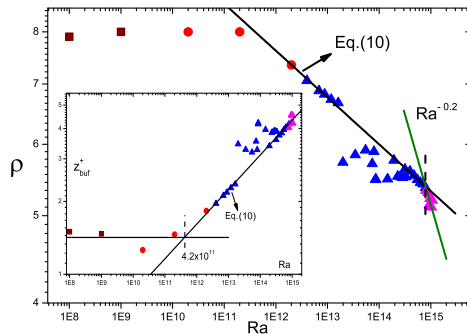


FIG. 3: (color). The variation of the two model parameters, ρ (main) and z_{buf}^+ (inset), as a function of Ra , derived using (8) and (9) from DNS data: brown squares (our data), red discs [1], blue and purple triangles (experimental data [1]). Interpretations: for $Ra < 4.2 \times 10^{11}$, the measuring point ($x = 0.0045$) is located within the sidewall kinetic boundary layer; for $Ra > 4.2 \times 10^{11}$, the measuring point experiences strong turbulence of the "classical regime", governed by (10); for $Ra > 8 \times 10^{14}$, the ultimate regime [6] is characterized by $\rho \propto Ra^{-0.2}$.

We thank G. Ahlers and E. Bodenschatz for discussions and for sharing data. This work is supported by National Nature Science Fund 90716008 and by MOST 973 project 2009CB724100.

-
- [1] G. Ahlers, E. Bodenschatz, et al, Phys. Rev. Lett. 109, 114501 (2012).
 - [2] Procaccia, I., E. S. C. Ching, et al, Phys. Rev. A 44, 8091-8102(1991).
 - [3] L.P. Kadanoff, Phys. Today 54 (8), 34-39 (2001).
 - [4] G. Ahlers, S. Grossmann, D. Lohse, Rev. Mod. Phys., 81, 503 (2009).
 - [5] D. Lohse, K.-Q. Xia, Annu. Rev. Fluid Mech. 42, 335 (2010).
 - [6] X. He, D. Funfschilling, E. Bodenschatz, G. Ahlers, New J. Phys. 14, 063030(2012).
 - [7] G. Ahlers, X. He, D. Funfschilling, E. Bodenschatz arXiv:1205.0108(2012).
 - [8] X. He, D. Funfschilling, et al, Phys. Rev. Lett. 108, 024502 (2012).
 - [9] S. Grossmann, D. Lohse, Phys. Fluids 23, 045108 (2011); S. Grossmann, D. Lohse, arXiv:1208.2597(2012).
 - [10] S. Grossmann, D. Lohse, J. Fluid Mech. 407, 27-56 (2000).
 - [11] Z.S. She, X. Chen, Y. Wu, F. Hussain, Acta Mech Sinica, 26, 847-861 (2010); Z.S. She, X. Chen, F. Hussain, arXiv:1112.6312(2012).
 - [12] Z.S. She, X. Chen, Y. Wu, F. Hussain, arXiv:1112.6310 (2012); X. Chen, F. Hussain, Z.S. She, arXiv:1209.4154 (2012).
 - [13] Siggia, E. D., Annu. Rev. Fluid Mech. 26, 137-168 (1994).
 - [14] L'vov V.S., Procaccia I., Rudenko O., Phys. Rev. Lett. 100, 054504(2008).
 - [15] F. Heslot, B. Castaing, A. Libchaber Phys. Rev. A 36, 5870-5873(1987).
 - [16] S.Q Zhou, K.-Q. Xia, Phys. Rev. Lett. 89, 18 (2002)
 - [17] Q. Zhou, R. J. A. M. Stevens, et al, J. Fluid Mech. 664, 297 (2010).
 - [18] R.J.A.M. Stevens, Q. Zhou, et al, Phys. Rev. E. 85, 027301(2012).
 - [19] Z.S. She, Y. Wu, X. Chen, F. Hussain, New J. Physics, accepted (2012).
 - [20] Y.S. Zhang, W.T. Bi, F. Hussain, X.L. Li, Z.S. She, Phys. Rev. Lett. 109, 054502 (2012).